Stability of simple/complex classification with contrast and extraclassical receptive field modulation in macaque V1

Christopher A. Henry and Michael J. Hawken

J Neurophysiol 109:1793-1803, 2013. First published 9 January 2013;
doi: 10.1152/jn.00997.2012

J Neurophysiol 109: 1793–1803, 2013.
First published January 9, 2013; doi:10.1152/jn.00997.2012.

Stability of simple/complex classification with contrast and extraclassical receptive field modulation in macaque V1

Christopher A. Henry and Michael J. Hawken
Center for Neural Science, New York University, New York, New York

Submitted 15 November 2012; accepted in final form 2 January 2013

Henry CA, Hawken MJ. Stability of simple–complex classification with contrast and extraclassical receptive field modulation in macaque V1. *J Neurophysiol* 109: 1793–1803, 2013. First published January 9, 2013; doi:10.1152/jn.00997.2012.—A key property of neurons in primary visual cortex (V1) is the distinction between simple and complex cells. Recent reports in cat visual cortex indicate the categorization of simple and complex can change depending on stimulus conditions. We investigated the stability of the simple/complex classification with changes in drive produced by either contrast or modulation by the extraclassical receptive field (eCRF). These two conditions were reported to increase the proportion of simple cells in cat cortex. The ratio of the modulation depth of the response (F1) to the elevation of response (F0) to a drifting grating (F1/F0 ratio) was used as the measure of simple/complex. The majority of V1 complex cells remained classified as complex with decreasing contrast. Near contrast threshold, an equal proportion of simple and complex cells changed their classification. The F1/F0 ratio was stable between optimal and large stimulus areas even for those neurons that showed strong eCRF suppression. There was no discernible overall effect of surrounding spatial context on the F1/F0 ratio. Simple/complex cell classification is relatively stable across a range of stimulus drives, produced by either contrast or eCRF suppression.

primate V1; simple and complex cells; contrast; extraclassical receptive field

NEURONAL RECEPTIVE FIELDS underlie perceptual interpretation of the visual world. The most important receptive field dichotomy in visual cortex is between simple and complex cells (Hubel and Wiesel 1962). Simple cells are central in signaling the position and sign of oriented luminance and chromatic border segments. Complex cells do not provide signals that are strongly sensitive to position and sign of luminance edges. Some recent studies report that the classification of neuronal populations into simple and complex cells is dependent on the stimulus conditions prevailing during categorization (Bardy et al. 2006; Crowder et al. 2007; van Kleef et al. 2010). The potential lability of the simple/complex categorization has major implications for understanding how processing proceeds in the visual pathway. If members of the neuronal population dynamically change their fundamental properties depending on the properties of the visual scene, then circuit and computational models will need to take into account the scene-dependent nature of processing within the visual pathway.

Hubel and Wiesel showed that neurons in primary visual cortex of both cat (1962) and primate (1968) could be classified as simple or complex. There are a number of features of the receptive fields of simple and complex cells that differentiate them; one that has been adopted in many studies is the ratio of the modulated to unmodulated response to drifting grating stimuli, the F1/F0 ratio (Skottun et al. 1991). Furthermore, the F1/F0 ratio has been shown to correlate strongly with other traditional measures of the receptive field properties of simple and complex cells, such as summation within and spatial separation between subfields (Dean and Tolhurst 1983; Mata and Ringach 2005). Recent studies in cat visual cortex reported that the F1/F0 ratio was dependent on the nature of the visual stimulus (Bardy et al. 2006; Crowder et al. 2007; van Kleef et al. 2010), making the distinction between the simple and complex neurons a dynamic classification based on stimulus conditions. When the responses of neurons were probed with a low contrast stimulus, or when the suppressive surround was activated in neurons that showed extraclassical receptive field (eCRF) suppression, then complex cells became more "simple-like," whereas few simple cells changed their classification (Bardy et al. 2006; Crowder et al. 2007). This means that the F1/F0 ratios of neurons classified as complex on the basis of high-contrast stimuli or with stimuli restricted to their classical receptive fields (CRF) tend to increase with suboptimal stimuli such that some complex cells change category and become reclassified as simple cells. These results have important implications for understanding how receptive fields are generated and how cortical circuits operate.

We sought to determine if the classification of simple and complex cells in primate visual cortex was similarly stimulus dependent as it was reported to be in cat visual cortex, hence testing the generality, across species, of the dynamic nature of receptive field properties. Experiments were performed in the primate visual cortex using stimulus paradigms intended to differentially alter thalamocortical and intracortical activity to examine their influence on neurons' F1/F0 ratios. It has been reasoned that changing the contrast of a small, spatially restricted stimulus will be effective in altering the relative ratio of the drive from the lateral geniculate nucleus (LGN) to the cortex compared with the intracortical drive (Chance et al. 1999). Consequently, it has been proposed that complex cells should become more simple-like at low contrast (Crowder et al. 2007), particularly in the thalamic recipient zones layers 4c and 6. To test this reasoning, we measured the F1/F0 ratio at different contrasts for stimuli in patches restricted to the CRF as a means of changing responses with a dominant thalamocortical component. In addition, many V1 neurons suppress their responses to an optimal stimulus when it is either increased in size or embedded in a spatially extended context. Most, but not all, of the suppression in the eCRF is orientation dependent (Cavanaugh et al. 2002b; DeAngelis et al. 1994; Levitt and Lund, 1997; Xing et al. 2005) and exhibits intero-

Address for reprint requests and other correspondence: M. J. Hawken, Center for Neural Science, New York Univ., 4 Washington Place, Rm. 809, New York, NY 10003 (e-mail: mjh2@nyu.edu).

cular transfer in most binocular cells (DeAngelis et al. 1994; Webb et al. 2005), which suggests a cortical origin. We used eCRF suppression to determine the effects on the F1/F0 ratio of changing the response via a dominant cortical component. To test whether effects from the eCRF were orientation dependent, we used stimuli that were at both collinear and orthogonal orientations relative to the preferred orientation in the CRF.

There was little effect of contrast on the F1/F0 ratio in macaque V1. As a population, the majority of macaque V1 cells classified as complex with a high-contrast stimulus did not tend to become significantly more simple-like with decreasing contrast. Of the minority of neurons that did change, approximately equal proportions of complex cells became simple-like and simple cells became complex-like. Furthermore, the F1/F0 ratio was also remarkably stable with changes in stimulus size, even for those neurons that showed strong eCRF suppression. There was no discernible overall effect of surrounding spatial context on the F1/F0 ratio. In summary, receptive field organization at the level of the simple/complex cell dichotomy appears to be largely invariant with stimulus conditions in monkey V1.

MATERIALS AND METHODS

Preparation

Adult male old-world monkeys (*M. fascicularis*) were used in acute experiments in compliance with National Institutes of Health and New York University Animal Use Committee regulations. The animal preparation and recording were performed as described in detail previously (Hawken et al. 1996; Ringach et al. 2002; Xing et al. 2005). Anesthesia was initially induced using ketamine (5–20 mg/kg im) and was maintained with isoflurane (1–3%) during venous cannulation and intubation. For the remainder of the surgery and recording, anesthesia was maintained with sufentanil citrate (6–18 $\mu g \cdot kg^{-1} \cdot h^{-1}$ iv). After surgery was completed, muscle paralysis was induced and maintained with vecuronium bromide (Norcuron, 0.1 $mg \cdot kg^{-1} \cdot h^{-1}$ iv) and anesthetic state was assessed by continuously monitoring the animals' heart rate, ECG, blood pressure, expired CO_2, and EEG. At the end of recording sessions, animals were deeply anesthetized with pentobarbital sodium (60 mg/kg iv) and were transcardially exsanguinated with heparinized lactated Ringer, followed by 4% paraformaldehyde in 0.1 M phosphate buffer (pH 7.4). Electrode penetrations were located in histological sections, and layer assignment of recorded neurons was carried out as described previously (see Hawken et al. 1988; Ringach et al. 2002).

Characterization of Visual Properties of V1 Neurons

We recorded extracellularly from single units in V1 using glass-coated tungsten microelectrodes. Action potentials were discriminated using custom software running on a Silicon Graphics O2 and time stamped at a resolution of 0.1 ms. We identified single-unit activity using the criteria of a fixed action potential shape and an absolute refractory period between individual action potentials. Each single neuron was stimulated monocularly through the dominant eye (with the nondominant eye occluded). The steady-state response to drifting gratings was determined to provide an initial characterization of visual response properties. The initial measurements were orientation tuning, spatial and temporal frequency tuning, contrast response with achromatic gratings, and color sensitivity followed by area summation and annulus summation curves. Receptive fields were located at eccentricities between 1° and 6°. Stimuli were presented using custom software on either a Sony Trinitron GDM-F520 CRT monitor (mean luminance 90–100 cd/m^2) or an Iiyama HM204DT-A CRT monitor (mean luminance 60 cd/m^2). The monitors' luminance was calibrated using a spectroradiometer (Photo Research PR-650) and linearized via a lookup table using custom software. Stimuli were displayed at a screen resolution of 1,024 × 768 pixels, a refresh rate of 100 Hz, and a viewing distance of 115 cm.

The following three experiments were used for evaluating the stability of neurons' cellular classification (simple vs. complex) under dynamic changes in visual stimulation.

Contrast response. The response as a function of contrast was determined for contrasts ranging from 2 to 100% in 0.5-octave steps (Fig. 1*A*). A blank condition (screen of mean gray luminance) of the same duration as the stimulus presentation was shown at the beginning of each sequence and interleaved between each contrast presentation. The contrasts were shown in ascending order to avoid adaptation and to minimize hysteresis (Bonds 1991). Each grating presentation lasted for a minimum of four temporal cycles, often more, and was at least 1 s in duration. At least three repeats of the contrast sequence were given. Neurons that fired a mean stimulus-driven rate of at least 5 spikes/s above their spontaneous activity and had identified laminar locations were selected for subsequent analysis of their contrast-response functions.

Area summation. The response was measured as a function of stimulus area for a circular patch of grating of optimal spatial frequency, temporal frequency, orientation, and direction of drift at a contrast of about 90% of the contrast that produced the maximum response (Fig. 1*B*). Initially, the center of the CRF was estimated by moving an optimal drifting grating with a small aperture (usually 0.1–0.2° in radius) until the maximum discharge rate was judged by the experimenter. The patches of grating were centered on the *x, y* coordinates of the CRF center. A range of sizes from 0.05 or 0.1° up to 4° in radius were shown; the step between successive sizes was a factor of $\sqrt{2}$ (0.5 octave). Stimuli were shown in pseudorandom order for each repeat of the sequence. The number of repeats was at least three. A blank stimulus, the same duration as the stimulus, was shown between each repeat.

Spatial context. An optimal stimulus was shown in a stimulus patch covering the CRF while a second grating was shown in the eCRF. The size of the CRF was estimated from the area summation experiment (Fig. 1*B*) and taken as the radius of the smallest stimulus that produced the maximal response. For area summation functions that showed suppression at larger areas, this value was the radius that gave the peak response; if there was no suppression, it was the smallest radius where the response first reached about 90% of the maximum response. The inner border of the eCRF region was determined in an

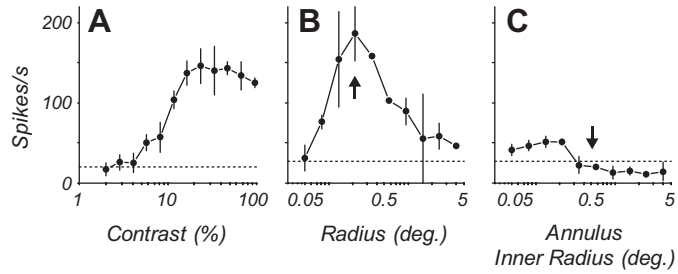

Fig. 1. Contrast response, area summation, and annulus tuning for an example complex cell. *A*: contrast-response function for a stimulus confined to the classical receptive field (CRF). *B*: area-response function with a stimulus of preferred spatiotemporal frequency and direction of drift. The size of the stimulus in the CRF was chosen to be the smallest size evoking the optimal response (vertical arrow). *C*: response as a function of the size of an annular region of optimal grating. The central mean gray area of the stimulus expands as the inner radius of surround grating increases. The stimulus at zero inner radius is equivalent to the largest radius in *B*. As the inner radius increases, the response decreases until there is no response from the CRF (vertical arrow). This is the inner radius chosen for the extraclassical receptive field (eCRF) context experiments. All points are means ± SD.

annular summation experiment, where the response was measured as a function of the diameter of the mean gray region in the center of an 8°-diameter square patch of grating (Fig. 1*C*). As the central gray patch's diameter increased, the width of the outer annular grating region decreased correspondingly. This annular summation experiment was used to determine the size of the inner radius of the eCRF region, the region where no response was elicited from the surround region when the center was masked by a gray region (Cavanaugh et al. 2002a). This is the region beyond the radius marked by the vertical arrow in Fig. 1*C*. We used the data collected from these two summation experiments to determine the size of the stimuli in the subsequent experiments. In the contextual modulation experiments the radius of the stimulus for the CRF was chosen to be the radius that evoked the peak response in the area summation experiment, shown by the vertical arrow at a radius of 0.2° in Fig. 1*B*. The eCRF stimulus was an annular region with an outer radius of 8° and an inner radius derived from the annular summation experiment, shown by the vertical arrow at a radius of 0.5° in Fig. 1*C*. The outer radius of the center stimulus was always smaller than the inner radius of the surround region, and the annular region between these two stimulus areas was mean gray.

To measure response modulation (F1/F0 ratio) in the CRF in the presence of stimuli in the eCRF, an optimal stimulus, at a contrast eliciting 90% of the neuron's maximum response, was presented to the CRF simultaneously with gratings of different contrast and orientation confined to the eCRF. Gratings in the eCRF were presented at collinear, orthogonal, and opposite directions of motion relative to the central stimulus patch, across contrast ranges from 5 to 80% in octave steps.

Data Analysis

Modulation analysis. For all conditions, responses were the mean firing rate (F0) taken over the duration of the stimulus presentation, and the amplitude of the first harmonic response (F1). The spontaneous baseline firing rate was subtracted from the stimulus-driven F0 component before the F1/F0 ratio was computed. The drift rates of the grating in the CRF and eCRF regions were always the same and were set to the optimal temporal frequency for the CRF alone assessed from a temporal frequency-response tuning function. To generate error bounds on the F1/F0 ratio for each condition, a bootstrap analysis was performed in which we randomly sampled (with replacement) from the set of responses to each temporal cycle of the stimulus and computed the F1/F0 ratio on this resampled data. This was repeated 10^6 times to generate an empirical distribution of the F1/F0 ratio for each stimulus condition. Significance tests for stimulus-dependent changes in the F1/F0 ratio were conducted on these empirical distributions in the following manner. Comparisons were made between draws from the F1/F0 distributions for two stimulus conditions; this procedure was repeated a large number of times (10^6), and comparisons were reported as significant when one value was greater at least 95% of the time. An additional test was carried out since, for a finite number of stimulus repeats, a lower average firing rate is positively correlated with an increase in the measured F1 component of the response, even for an entirely random process (Crowder et al. 2007). Thus, for each data set, we generated an artificial data set containing the same distribution of firing rates across stimulus cycles as the original, but within each cycle the spike times were uniformly distributed. Bootstrapping of this artificial data set gave us a distribution of F1 components with which to test whether a given stimulus condition elicited an F1 component of the response significantly greater than that of a "rate-equated" random process.

Contrast response. The F1/F0 modulation ratio was compared at low and high contrast relative to the contrast-response function for each neuron. Because neurons differed in their contrast-response functions, the low and high contrasts for the analysis of the F1/F0 ratio were chosen on the basis of the individual contrast-response functions. Each neuron's contrast threshold was determined to be the lowest contrast in which the average firing rate was significantly greater ($P < 0.05$) than the spontaneous activity. Across the population, the F1/F0 ratio was estimated for threshold contrast, $\sqrt{2}$ times threshold, two times threshold contrast, and high (90–99%) contrasts. In the few neurons that showed supersaturation at high contrasts, the F1/F0 ratio at the highest contrast was similar to that at the stimulus contrast evoking the maximum response.

RESULTS

The contrast-response function was determined for 462 neurons from all layers of V1. The F1/F0 ratio was calculated at each level of contrast from threshold to high contrast, and it was determined whether the F1/F0 ratio changed as a function of contrast. Next, the response was measured as a function of stimulus area, and the F1/F0 ratio was determined as a function of area for 66 neurons. Finally, the response to a constant stimulus in the CRF was measured for gratings with collinear, orthogonal, and opposite directions of drift in the eCRF. A comparison of the F1/F0 ratio was made between these different eCRF stimulus conditions for 47 neurons.

Changing Stimulus Contrast

For each neuron the mean response amplitude (F0) and the amplitude of the first harmonic (F1) at the same temporal frequency as the drift rate were determined. Neurons classified as simple based on F1/F0 > 1 showed a substantial modulation of their firing rate at the same temporal rate as the stimulus modulation (Fig. 2*A*, example simple cell). Neurons that were classified as complex based on F1/F0 < 1 increased their response as contrast increased without substantial modulation at the stimulus drift rate, although some cells showed a small modulation along with the unmodulated increase in discharge (Fig. 2*D*, example complex cell). We determined whether the F1/F0 ratio changed as a function of stimulus contrast. The F1/F0 ratio for the example complex cell was invariant with contrast (Fig. 2, *E* and *F*). The simple cell showed a larger F1 than F0 response at high contrast (Fig. 2*B*; F1/F0 ratio 1.54). The response developed at relatively low contrast, around 4%, but rose without showing significant saturation. The cell's F1/F0 ratio remained constant across all contrasts that elicited a response (Fig. 2*C*). The maintained discharge rate of the complex cell rose from a threshold of about 3% contrast to saturate at just about 10% contrast (Fig. 2*E*, solid black line). The F1 modulation amplitude was small in this neuron at the highest contrast and remained relatively low across all contrasts (Fig. 2*E*, dashed gray line). For most neurons, at a contrast twice threshold there was a robust and reliable response even though this contrast was near the lower region of the contrast response function. Therefore, we compared the F1/F0 ratio at twice threshold contrast and high contrast for the entire population of 462 neurons tested. High contrast was the highest contrast that was used for determining the contrast-response function; it was greater than 90%, typically 96% or 99%.

Figure 3 shows a summary of F1/F0 ratio comparisons between high and low (2 times threshold) contrasts for both complex (Fig. 3*A*) and simple (Fig. 3*B*) cell populations as classified on the basis of responses to a high-contrast stimulus. As a population, there was a statistically significant difference

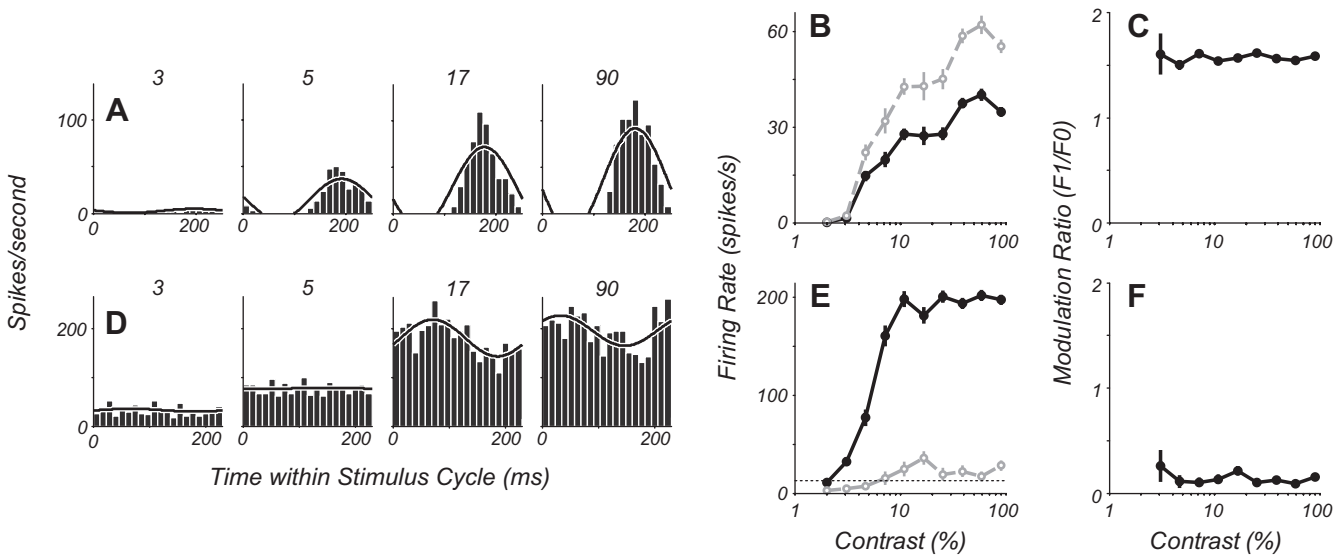

Fig. 2. Contrast-response data from example simple (*A–C*) and complex cells (*D–F*). *A* and *D*: peristimulus time histograms (PSTHs) to 1 stimulus cycle are shown for 4 stimulus contrasts. The black line shows the half-wave rectified sum of the zeroth and first harmonic of the Fourier transform of the responses. *B* and *E*: firing rates as a function of contrast for both the F0 (solid black line) and F1 (dashed gray line) components of the response (means ± SE). *C* and *F*: the ratio of the F1/F0, the modulation ratio, shown as a function of contrast (mean ± SE), does not change systematically as a function of increasing contrast.

in F1/F0 measures at the two contrasts for both complex ($P < 0.001$) and simple cells ($P < 0.006$, Wilcoxon signed-rank test). However, for both cell classes, the modulation ratio of the majority of neurons did not significantly change in response to lowered luminance contrast of the stimulus [78% (180/230) of complex cells and 63% (146/232) of simple cells]. Significance testing of individual neurons for changes in F1/F0 was based on a bootstrap analysis (see MATERIALS AND METHODS). For those simple cells that showed a change in their modulation ratio (Fig. 3*B*, black circles), the proportions of cells showing an increase (18%, 41/232) vs. a decrease (19%, 45/232) were about equal. The complex cells that did change their ratios significantly tended to show an increase at low contrasts. However, as described in MATERIALS AND METHODS, even an entirely phase-invariant neuron would show a relatively larger F1 component of the response to a stimulus of lowered contrast, purely due to the overall decrease in firing rate. For this reason, we compared each neuron's F1 response to that of a random process with equal numbers of spikes to determine whether each neuron produced a significant F1 component of the response. Overall, 17% (40/230) of complex cells showed an increase in F1/F0 ratio at low contrasts, with 13% (30/230) showing a significant F1 component (Fig. 3*A*, black circles). A comparison of complex cells' F1/F0 ratios at high contrast showed those cells that significantly increased their modulation ratios at low contrast had significantly higher F1/F0 ratios at high contrast compared with those cells that did not show significant increases at low contrast ($P < 0.002$, Wilcoxon rank-sum test). The 13% of complex cells that did show significant changes in F1/F0 with contrast and significant F1 components in their responses tended to have F1/F0 ratios nearer 1 than the overall complex cell population. The change in phase sensitivity near threshold constituted a small shift in the population response, but the majority of neurons (87%) did not change significantly. Thus it seems unlikely that there will be an overall alteration in the cortical representation of visual information with changing contrast.

Proportion of cells that changed their simple/complex classification. The majority [78% of complex cells (Fig. 3*A*) and 63% of simple cells (Fig. 3*B*)] of the V1 neurons in our sample had stable modulation ratios in response to stimuli of both high contrast and a lower contrast that was twice the neuron's contrast threshold. Within the complex cell population that showed significant changes in the F1/F0 ratio, only 7% (17/230) crossed the category boundary from a ratio of <1 to a ratio of >1 so that they would be classified as simple cells at low contrast. The histograms in Fig. 3 illustrate the distribution of F1/F0 ratios across a broad range of contrasts for simple (Fig. 3, *G–J*) and complex cells (Fig. 3, *C–F*), as classified on the basis of high-contrast stimuli. Across most of the neurons' operating ranges, the F1/F0 distributions remained similar to those at high contrast; only those distributions of simple and complex cells at contrast threshold appeared markedly different (Fig. 3, *F* and *J*). Responses at contrast threshold were by definition weak, and measurement noise needs to be considered. Whereas 32% (73/230) of complex cells showed an increase in F1/F0 at contrast threshold, only 5% (12/230) showed a significant F1 component in their response. Thus the apparent shift in F1/F0 distribution at contrast threshold was largely a consequence of elevated estimates of the F1 component due to low firing rates and finite data, and the shift would be similar for a model, phase-invariant neuron.

The comparison of responses based on stimulus contrast relative to threshold gave a picture of the magnitude of the neural response without taking into account gain or slope of the contrast-response function for individual neurons. A given suprathreshold contrast could have elicited a saturated response in one neuron while only eliciting an intermediate response in another if there was a difference in the gain of their contrast-response functions. To account for differences in intrinsic drive, the normalized driven response was calculated for each neuron and each stimulus by subtracting the spontaneous firing rate from all stimulus-driven responses and then taking the

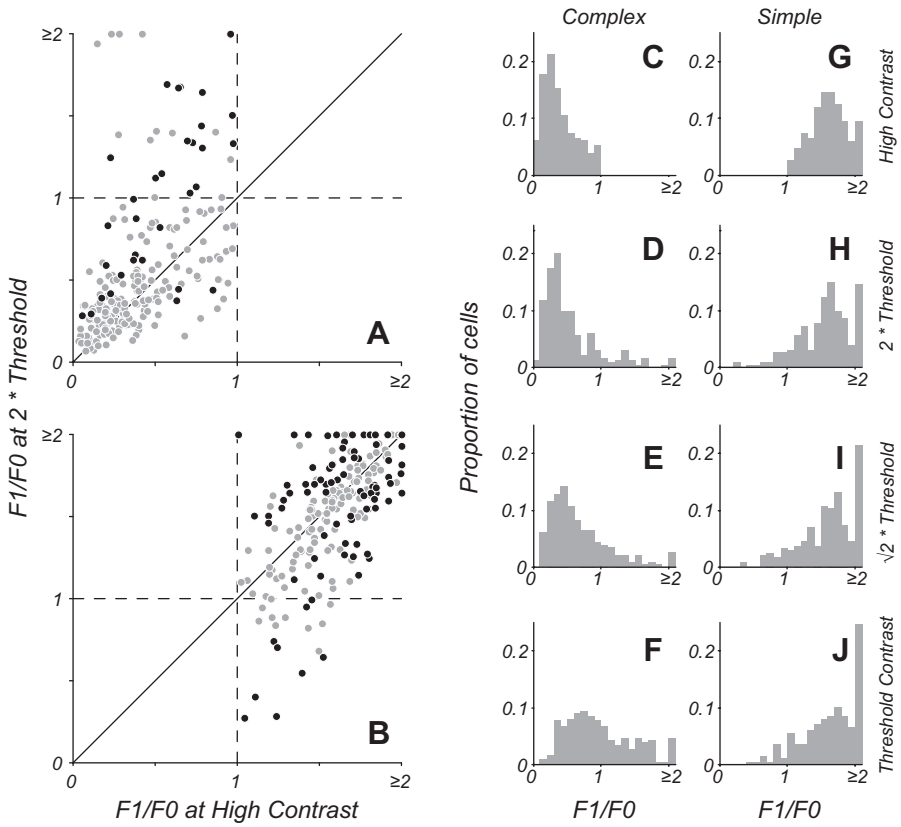

Fig. 3. F1/F0 ratio for the population at different contrast levels. *A* and *B*: F1/F0 ratio measured at high contrast (*x*-axis) plotted against the ratio at a low contrast that is twice threshold (*y*-axis). The gray points show neurons that do not significantly change their modulation ratio. Black points show neurons that have a significant change in ratio; for complex cells (*A*), the black points indicate the subset of cells that had both a significant change in ratio and a significant F1 component in their response. There is a small increase in the F1/F0 for some complex (F1/F0 < 1) cells, but overall the ratio remains relatively constant (*A*). For simple cells (F1/F0 ratio > 1), the majority do not show a significant change, but a small number increase or decrease their ratio (*B*). *C–J*: the histograms show F1/F0 ratios for cells classified as simple or complex on the basis of high-contrast stimuli. The high-contrast distributions are shown in the *top* row (*C* and *G*); the lower rows show distributions for the complex and simple cells classified at high contrast. The distributions of F1/F0 for complex and simple cells remain similar as contrast is lowered to twice threshold (*D* and *H*) and $\sqrt{2}$ times threshold (*E* and *I*), but a small proportion of the population change their classification. There is an average increase in F1/F0 for complex cells at contrast threshold (*F*), but this is largely due to low firing rates (see RESULTS); only a small fraction of neurons (5%) possess an F1 component that is significantly greater than that produced by a model phase-invariant neuron firing at the same low mean rate. *J*: simple cells as a population show a similar distribution at threshold as at higher contrasts.

ratio of the response at the chosen contrast over that of the response at the highest contrast presented. This procedure gave a normalized measure whereby a response of 1 was similar to the neuron's response at high contrast, and a response close to 0 was near the neuron's firing threshold (note: this normalized measure exceeded a value of 1 when the maximum response was to a contrast lower than the highest contrast). Figure 4 shows population data on how the modulation ratio changed at given contrasts relative to high contrast as a function of the amount of drive that each contrast provided to the neurons. Data points are included from each neuron for all conditions in which the stimulus contrast is above the neuron's contrast threshold. For simple cells, on average the modulation ratio showed no systematic deviation across the operating range of the neurons (Fig. 4*B*). For complex cells (Fig. 4*A*), the modulation ratio was relatively unchanged across most of the operating range (25% of the maximum response and higher) but increased and became more simple-like in the range near firing threshold (0–25% of the maximum response). The running average of all data points is shown in Fig. 4, *A* and *B* (solid black line, mean change; shaded gray region, ±SD). Analysis of neurons' responses at low contrast showed that the elevation in F1 was often a consequence of low spike rates (or drive) and not significantly different from a random process with a matched low spike rate (see MATERIALS AND METHODS). Data for stimulus conditions in which complex cells showed a significant F1 component of their response along with a significant change in F1/F0 ratio are plotted as black data points in Fig. 4*A*. Although in the majority of stimulus conditions complex cells showed no significant change in the F1 component of their response (gray data points), many showed an increase in F1/F0 ratio at low drive due to lowered average firing rates. For most of the operating range (>25% maximum firing rate), both simple and complex cells' modulation ratios remained relatively constant, indicating that the stimulus-related F1/F0 measure of spatial phase selectivity of the neural population as a whole was stable across substantial changes in stimulus contrast.

Although the population of simple cells showed no systematic changes in modulation ratio on average, subpopulations of simple cells showed significant increases or decreases in modulation ratio at lowered contrasts. To determine whether these changes in modulation ratio were systematic and reliable across contrast, we compared the responses of simple cells that

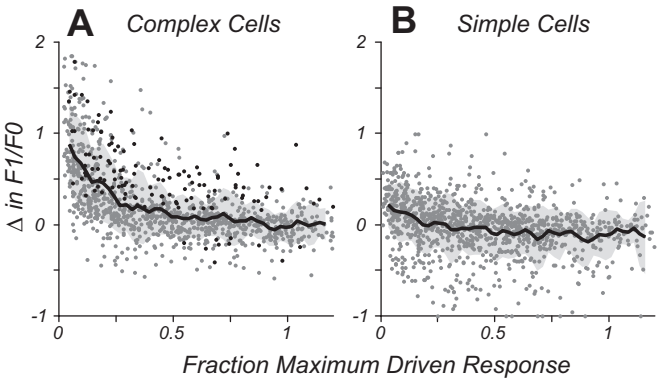

Fig. 4. Population data showing how the change in F1/F0 ratio is related to the amount of response drive (normalized to the individual neuron's firing rate at high contrast). *A*: complex cells show little change in F1/F0 across 75% of their operating range (0.25–1) but increase at firing rates below 25% of the maximum response. Points in black show cells and conditions with a significant change in F1/F0 and a significant F1 component to the response. For a majority of cases, the increase in F1/F0 ratio at low drive is not significant and is due to the low firing rate. The solid black line shows the running average of all data points (gray-shaded region, ±SD) using a boxcar of 0.05 width. *B*: simple cells, as a population, show no systematic change in F1/F0 on average across their operating range.

showed significant changes at a contrast twice threshold with those same cells' responses at the next higher contrast tested ($2\sqrt{2}$ above threshold). Figure 5*A* plots these data for simple cells showing both significant increases (black) and decreases (gray) in modulation ratio. Changes in modulation ratio were correlated across neighboring contrasts ($P < 0.001$) for both subclasses of cells, indicating that these changes were consistent. Furthermore, for both groups of cells, observed changes in modulation ratio were lower at the contrast $2\sqrt{2}$ times threshold compared with 2 times threshold, as would be expected if lowering contrast introduced systematic changes in F1/F0 ratio compared with high contrast. Figure 5*B* shows that the relative amount of change in modulation ratio at low contrast was correlated with neurons' modulation ratios at high contrast ($P < 0.001$); cells with F1/F0 near 1 at high contrast showed larger proportional changes in modulation ratio than cells with F1/F0 near 2 at high contrast. For the subpopulations of simple

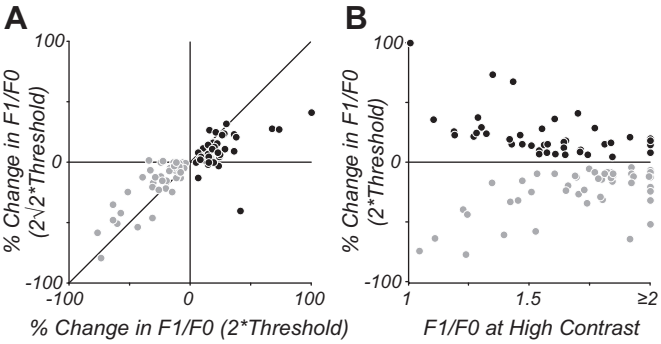

Fig. 5. Analysis of the change in F1/F0 ratio shown by simple cells at different contrast levels. *A*: change in F1/F0 at twice threshold is plotted against change at $2\sqrt{2}$ times threshold for simple cells, showing significant increases (black) and decreases (gray) in modulation ratio. The changes are correlated across contrasts and systematically lower at higher contrast, indicating a consistent bias for a change in F1/F0 at lower contrasts. *B*: changes in F1/F0 at twice threshold for the same cells in *A* are plotted in relation to the cells' modulation ratio at high contrasts. Cells with a F1/F0 near 1 tend to show larger relative changes at low contrast compared with cells with F1/F0 near 2.

cells that either increase (41/232) or decrease (45/232) their F1/F0 ratio at threshold contrast compared with high contrast, the direction of the change was the same at twice threshold and at $2\sqrt{2}$ times threshold, indicating the change was robust in these subpopulations. The degree of change in the F1/F0 ratio for the majority of simple cells that had significant changes in their F1/F0 ratio was relatively small (<25%). Because most simple cells' F1/F0 ratios were distributed around the ratio of 1.57 (characteristic of a half-wave rectification) at high contrast, a small change meant that only 4% (9/232) of simple cells significantly decreased their F1/F0 ratio to below 1 and would consequently be reclassified as complex at lower contrasts that are twice their threshold.

Laminar organization. The analyses shown so far have pooled data across all cortical layers. Neurons' response properties often differ markedly with regard to their laminar location and place within the cortical circuit. The separate layers of primary visual cortex differ with regard to their feedforward (thalamocortical) and recurrent (intracortical) connectivity, with the strongest LGN input in macaque V1 found in layer 4c. To determine whether the differences in intralaminar circuitry lead to differences in stimulus-dependent classification of simple and complex cells in different layers, we analyzed the contrast data as a function of cortical layer. Figure 6 shows for simple and complex cells within each layer the proportion of cells whose F1/F0 ratio at low contrast (twice threshold) was either similar to (black) or significantly different from (gray) the F1/F0 ratio measured at high (>90%) contrast. For cells that did significantly change their ratio, the populations are further broken down into those that showed an increase (+) or a decrease (−) in F1/F0 ratio. Within each cortical layer, the

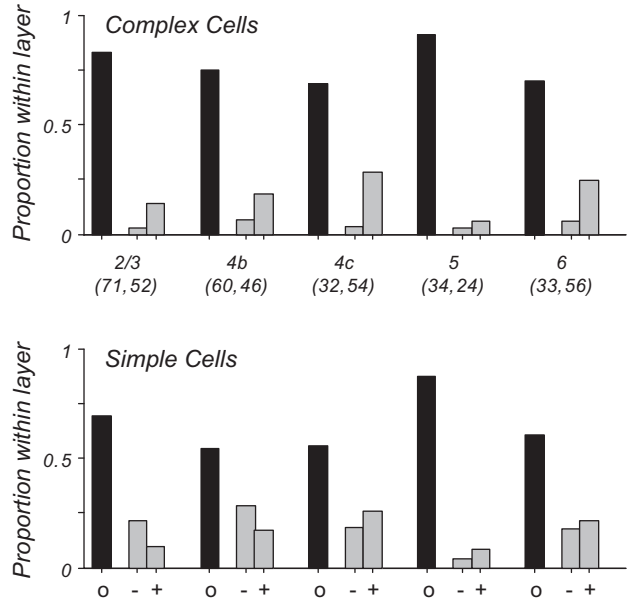

Fig. 6. Changes in F1/F0 with cortical layer based on measurements at twice threshold contrast compared with high contrast. Numbers in parentheses give the number of complex and simple cells, respectively, within each layer. Black bars indicate the proportion of cells in each layer showing no significant change in F1/F0 at lower contrast; gray bars represent the proportion of cells showing significant changes, for either increases (+) or decreases (−). The majority of cells in all layers show no significant changes in F1/F0 at lower contrasts. For both simple and complex cells, layers 2/3 and 5 have the most cells with stable F1/F0 ratios, and layer 4c shows the most cells with significant changes in modulation ratio.

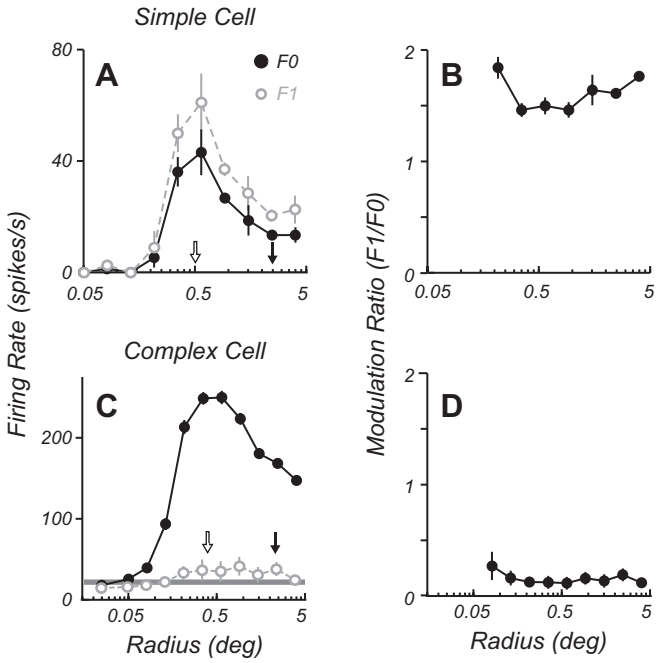

Fig. 7. Size tuning data for an example simple (*A* and *B*) and complex cell (*C* and *D*). Firing rates (*A* and *C*) are shown as a function of stimulus radius for F0 (solid black circles) and F1 (open gray circles) components of the response. Both neurons show an initial summation followed by a suppression at stimulus diameters beyond the optimal. The F1/F0 ratios (*B* and *D*) of both cells remain largely invariant with changing stimulus aperture. The optimal size (open arrow) and 2.5 times the optimal size (filled arrow) are shown in *A* and *C*.

majority of neurons did not show significant changes in F1/F0 at low contrasts, for both simple and complex cells (Fig. 6, black bars). Furthermore, comparison of the profile across layer shows a similar trend for both cell types; layers 2/3 and 5 showed the most stability in F1/F0, and layer 4c showed a greater tendency for changes in F1/F0 ratio with contrast. There was a significant difference in the proportion of neurons showing stable F1/F0 ratios across layers ($P < 0.001$, χ^2 test for equal proportions). For those cells that did change significantly, the trend across layers was similar to that seen in the scatter plots of Fig. 3; simple cells were equally likely to have an increase or decrease in F1/F0, and complex cells tended to have an increase in F1/F0, due at least in part to an effect of low firing rates.

Changing Stimulus Size

Studies in cat area 17 revealed that stimulation of the eCRF resulted in some complex cells changing their F1/F0 ratio, tending to show a higher ratio than when their CRF alone was stimulated. In the current study we compared the F1/F0 ratio for neurons using optimal stimulus spatial frequency, temporal frequency, orientation, and drift direction through circular apertures of different sizes. All neurons showed summation as the aperture size was increased until an optimal size was reached where the response was maximal (Fig. 7, *A* and *C*). Most neurons showed an attenuation of their response as the aperture was increased in size beyond the optimal (Fig. 1*B* and Fig. 7, *A* and *C*). For each neuron the optimal aperture size was determined from the area summation curve and the F1 and F0 of the response were determined for all stimulus sizes (Fig. 7, *A* and *C*). The F1/F0 response ratio for both example complex and simple cells remained relatively constant across aperture size (Fig. 7, *B* and *D*). To test the generality of this finding a comparison was made of the F1/F0 ratio at the optimal aperture size and the F1/F0 ratio for a stimulus aperture 2.5 times the optimal size (Fig. 8) for a population of neurons. Across the F1/F0 range there was no significant deviation from the equality line, shown by the moving average of the data in gray (Fig. 8). Neuronal firing rates were on average quite suppressed by the larger gratings (suppression index of 0.34 ± 0.23, mean ± SD), with the suppression index defined as $(R_O - R_N)/R_O$, where R_O is the response to an optimal stimulus and R_N is the response to a nonoptimal stimulus. However, there were no significant differences between the measures of F1/F0 at the two sizes for either simple or complex cells ($P > 0.6$ and $P > 0.1$, respectively, Wilcoxon signed-rank test). Finally, there was no correlation between the amount of suppression and the change in modulation ratio ($r = 0.19$, $P > 0.1$).

Changing Stimulus Context

One of the pronounced features of stimuli outside the CRF is that they provide a strong modulation of the response to an optimal stimulus inside the CRF, yet the stimulus in the nonclassical surround does not, itself, evoke a response. The area summation and annulus experiments were used to delineate the CRF and the eCRF (see MATERIALS AND METHODS). Four different experimental conditions were interleaved so that the response to a stimulus in the CRF alone could be compared with responses with stimuli copresented in the eCRF at collinear, orthogonal, or opposite directions of drift (Fig. 9*A*), to examine the effects of context on the F1/F0 ratio. In these experiments the major effect of presentation of a stimulus in the eCRF was contrast-dependent suppression, as shown for example simple (Fig. 9*B*) and complex cells (Fig. 9*C*). Contextual suppression was most often maximal for collinear stimuli. Nonetheless, the F1/F0 ratio was invariant with collinear stimulus context.

To analyze the population, we selected the stimulus context that gave the maximal suppression and then compared the

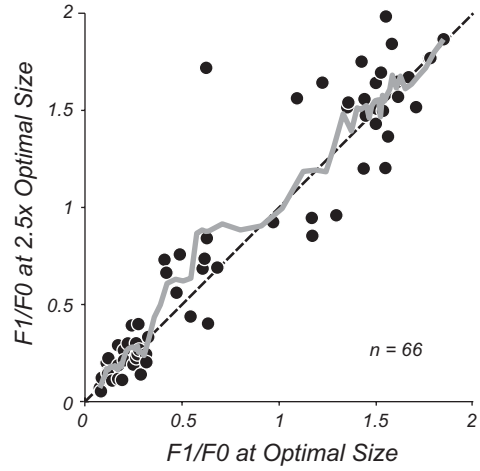

Fig. 8. A comparison of F1/F0 ratio measured at the optimal stimulus aperture (*x*-axis) plotted against the F1/F0 ratio for a stimulus aperture 2.5 times the optimal size. The solid gray line shows the running average (of the nearest 5 data points), which follows the line of equality (dashed black line). There is no systematic deviation of the ratio for either complex (F1/F0 < 1) or simple cells (F1/F0 > 1) when the size of the aperture is increased, even though for the majority of neurons there is response suppression in the larger size aperture.

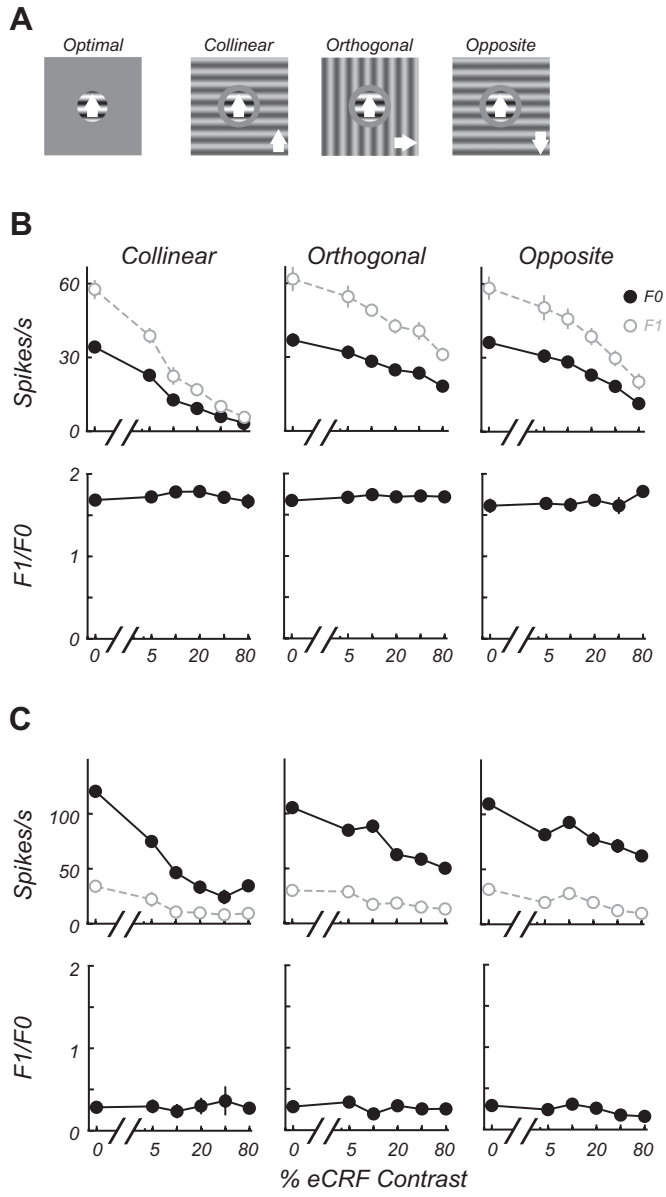

Fig. 9. Stimuli in the eCRF do not change the F1/F0 ratio. *A*: stimulus conditions for contextual experiments. Responses to an optimal grating confined to the CRF were compared with responses with stimuli presented simultaneously in the eCRF at collinear, orthogonal, and opposite directions of drift (indicated by white arrows) to the CRF grating. *B* and *C*: the response to an optimal stimulus in the CRF is modulated by different contextual stimulus configurations and contrasts in the eCRF for a simple (*B*) and a complex cell (*C*). The unmodulated F0 (filled black circles) and modulated F1 (open gray circles) components of the response are shown in each *top* graph (means ± SE, error bars are often obscured by the data points). For each condition the contrast of the stimulus in the eCRF was varied. The 0% contrast condition is the response to the stimulus in the CRF alone (*A*, optimal). The *bottom* graphs show that modulation (F1/F0) ratios for each condition remain invariant to manipulations of eCRF contrast and orientation that induce strong suppression.

F1/F0 ratios for the maximal suppression condition with the condition of stimulating only the CRF (Fig. 10). There was no difference in F1/F0 ratios between conditions across the population, as shown by the running average across all values of F1/F0 (Fig. 10, gray line); the modulation ratios remained stable despite the strong suppression caused by stimuli in the eCRF (suppression index of 0.48 ± 0.23, mean ± SD). Neither simple nor complex cells showed significant shifts in their modulation ratios in the presence of eCRF stimuli ($P > 0.2$ and $P > 0.4$, respectively, Wilcoxon signed-rank test). There was no correlation between the strength of suppression and changes in modulation ratio ($r = 0.16$, $P > 0.3$). Finally, none of the neurons classified as complex with an optimal stimulus switched their classification to simple due to changes in F1/F0 with eCRF suppression.

DISCUSSION

This simple/complex classification scheme, based on functional properties and receptive field structure (Hubel and Wiesel 1962), has been shown to be in strong agreement with a classification scheme based on the ratio of modulated (F1) to unmodulated (F0) responses to a drifting sinusoidal grating (Skottun et al. 1991). In the current study, we demonstrated that the modulation ratios of neurons in macaque V1 were generally stable across multiple changes in stimulus attributes. The stable F1/F0 ratio suggests that cell classification under optimal stimulus conditions generalizes well to neuronal responses under suboptimal stimulation conditions.

F1/F0 Invariance to Changes in Firing Rate

The F1/F0 ratios of most neurons remained constant despite large reductions in firing rate due to manipulations of the visual stimuli used to drive the cells. Moreover, this reduced drive was likely brought about through different neurophysiological mechanisms in the various experiments in this study. Lowering the contrast of a relatively small stimulus restricted to a neuron's CRF would likely produce a larger change in the feedforward thalamocortical drive compared with the recurrent drive via intracortical connections. Altering an optimal stimulus by increasing its size beyond the CRF or embedding it in a large spatially extended context will recruit both lateral and feedback connections intracortically. Regardless, in the face of manipulations that produced large decreases in stimulus-driven

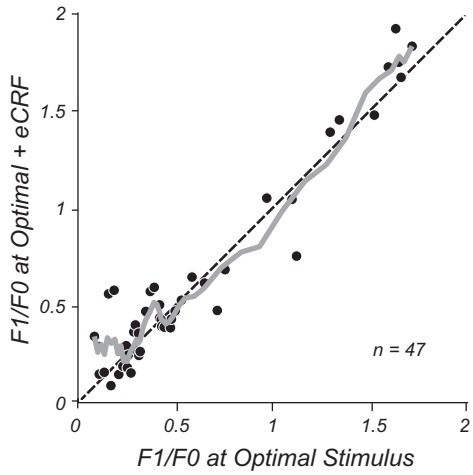

Fig. 10. F1/F0 ratios for the population measured with the optimal stimulus (*x*-axis) or the most suppressive contextual stimulus (*y*-axis) chosen across eCRF orientation, drift direction, and contrast from the experiments shown in Fig. 9. The solid gray line shows the running average (of the 5 nearest data points), which follows the line of equality (dashed black line). There is no systematic deviation of the ratio as the size of the aperture increases, even though for the majority of neurons there is a strong response suppression to the contextual stimulus in the eCRF.

firing rates, cortical circuitry appeared organized to keep neurons' modulation ratios relatively invariant to such changes in the network drive.

Studies in cat area 17 and 18 (Crowder et al. 2007) reported changes in F1/F0 for complex cells in all layers (2–6). However, they reported that a large proportion of their complex cells became "simple-like" at low contrasts, whereas only 13% (30/230) of our population showed increased modulation. Furthermore, Crowder et al. (2007) reported no changes in F1/F0 for their simple cell population, whereas we saw similar lability in F1/F0 with layer between simple and complex cells. Their study possessed a small sample (22/205, 11%) of simple cells. It is unclear whether Crowder et al.'s observed differences between simple and complex cells, unlike the lack of difference in the current study, were due to the small sample size of simple cells, pooling of neuronal populations across area (17 and 18), or a species difference. Our study in macaque V1 suggests that characterization of neurons on the basis of F1/F0 ratio is largely stable for simple and complex cells with similar dependency on location in the cortical circuit.

Consequence of Low Firing Rates

If the average firing rate dropped low enough, and given a finite number of stimulus presentations, even a simulated purely phase-invariant model neuron with no response modulation to a drifting grating showed an increase in F1/F0 ratio. This result occurred because as the mean number of spikes decreased, the ratio of first harmonic to mean increased, on average, simply due to chance. This result was fully laid out in a previous study (Crowder et al. 2007). We adopted the analysis method of Crowder et al. (2007) for determining whether a neuron's F1 response was significantly greater than that of a model phase-invariant neuron firing at the same mean rate. The majority of our complex cell population (200/230, 87%) did not show significant increases in their F1/F0 ratio with significant F1 responses as a function of lowered contrast, suggesting that, across the range of contrasts that neurons respond to, their responses to a sinusoidal grating were invariant with the spatial phase. For the small population of complex cells (13%) that significantly increased their F1/F0 ratio at low contrasts, the degree to which this increased phasic response impacts downstream cortical processing will be strongly dependent on the organization of convergent inputs. This increased phase sensitivity only occurred at low response rates near a neuron's firing threshold. If the neuron's responses were pooled with those of other neurons that have higher contrast sensitivities, the stronger responses would dominate in the pool. Furthermore, to the extent that a downstream neuron receives input from more than one complex cell, their increased phase biases at low contrast would have to be aligned in register for such contrast-dependent phase signals to propagate. Given the relatively small number of cells showing significant changes and the likely pooling of multiple V1 neurons in downstream receptive fields, we think such contrast-dependent phenomena are unlikely to play a major role in functional cortical processing. The fact that we observed even less lability in F1/F0 ratios for simple and complex cells in the major output layer 2/3 compared with that of the input layer 4c may be reflective of such convergent pooling of signals.

Comparison with Other Studies

In the past decade, many studies have challenged the strict hierarchical view of cortical organization originally proposed by Hubel and Wiesel in which simple cells are constructed out of LGN inputs and complex cells are formed by pooling inputs of V1 simple cells. One study (Alonso and Martinez 1998) recorded from complex cells that received direct monosynaptic input from the LGN. Furthermore, it has been shown both theoretically (Mechler and Ringach 2002) and experimentally (Priebe et al. 2004) that a sharply bimodal F1/F0 distribution of spiking responses can arise from a more uniform and unimodal distribution of underlying membrane potential responses, providing evidence for a more continuous, rather than discrete, view of cellular classification. Multiple studies using computational models of intracortical connectivity (Chance et al. 1999; Tao et al. 2004; Wielaard et al. 2001; Zhu et al. 2009) have shown ways in which the strength of recurrent intracortical activity can give rise to simple and complex cell classes. In such models, the degree of recurrent excitation is responsible for creation of complex cell responses; cells with stronger recurrent connectivity average over a greater number of inputs and produce more phase-invariant responses. Wielaard et al. (2001) demonstrated that a purely feedforward convergence of LGN inputs did not produce a linear receptive field (due to nonlinear distortion of LGN responses produced by the spiking threshold) and that intracortical inhibition in their model served to suppress these nonlinearities and created more linear simple-cell receptive fields. Interestingly, we showed that a proportion of simple cells responded differently to a stimulus of reduced contrast, with the cells that changed the most showing a decrease in F1/F0 ratio and more nonlinear behavior (Fig. 3*B*). In our study, similar proportions of simple and complex cells showed some stimulus-dependent influence on their F1/F0 ratios. Furthermore, not only were these proportions well-matched within each cortical layer, but they also differed across the cortical layers (Fig. 6), suggesting that the specific local intralaminar circuitry played some role in influencing this aspect of both simple and complex cell receptive fields.

Recent studies investigating the mapping of receptive field response properties with multiple stimulus sets have shown that the recovered spatiotemporal maps of V1 neurons can be strongly dependent on the mapping method and stimuli used (Sharpee and Victor 2009; Victor et al. 2009; Yeh et al. 2009). Basic receptive field properties in V1 such as orientation and spatial frequency tuning have been shown to be dynamically shaped by multiple mechanisms with varying spatial extents, thought to reflect aspects of the underlying anatomic (feedforward, recurrent) circuits (Xing et al. 2005). Given this, it is perhaps not surprising that receptive field maps may differ according to the method of visual stimulation. Stimulus sets that differ in luminance contrast, spatial resolution, visual extent, and correlational structure may provide differential drive to the multiple underlying functional circuits that shape a neuron's receptive field properties. It has been shown that neurons classified as simple or complex can be differentiated further with regard to temporal response nonlinearities and location within the cortical circuit (Williams and Shapley 2007; Williams et al. 2007), suggesting that subclasses of neurons may represent qualitatively different signals within the visual pathway. Studies in both anaesthetized (Mata and

Ringach 2005) and awake (Chen et al. 2009) macaque V1 have measured both F1/F0 responses to high-contrast drifting gratings as well as mapped receptive field overlap using sparse noise stimuli, which weakly drive a cell's receptive field and may be considered as a stimulus of low effective contrast. If complex cells' receptive field structure generally became more simple-like at low contrasts, we would expect either poor correlation or a strong bias between F1/F0 and measures of subunit discreteness or overlap, which neither study showed. This suggests that whereas other detailed receptive field measures may change with stimulus set, the basic organization of subunit separability or overlap may remain largely stable. In support of the stability of receptive field structure, a recent study in macaque V1 reported that static receptive field mapping with lower stimulus contrast did not appreciably alter the arrangement of RF subunits and that complex cells showed stability in their classification at low contrasts on the basis of subunit overlap (Durand et al. 2012).

Although we demonstrated that some cells of both classifications (simple and complex) did change their modulation ratio at lowered contrasts, we emphasize that the proportion is relatively small, that very few cells changed enough to be reclassified as the other type (7% of complex cells and 4% of simple cells), and that those cells that altered their F1/F0 ratios most tended to have intermediate F1/F0 values (0.7–1.3) when classified at high contrast, which is relatively uncommon in the population distribution as a whole (69/462, 15%). Recent studies in cat visual cortex (Crowder et al. 2007, van Kleef et al. 2010) reported that many complex cells become simple-like at low contrast, whereas simple cells showed no change in phase selectivity. It is unclear whether or not the difference between the current study in macaque and the studies in cat cortex are due to a species difference or some other factors. The study of Crowder et al. (2007) differed from ours in two respects: they sampled neurons from both area 17 and area 18 in the cat, and simple cells comprised only a small proportion of their overall sample population (22/205, 11%), whereas in our study half the neurons were simple (232/462, 50%) and the whole population was from V1. In the study of van Kleef et al. (2010), which recorded exclusively from area 17, only 10% of their complex cell population (8/77) became reclassified as simple at low contrast (Fig. 4*A*), whereas Crowder et al. found a proportion closer to ~50%. The results of van Kleef et al. (2010) resemble ours in that only a small minority of complex cells switched their classification to simple at low contrast, and these tended to be complex cells that already contained a moderate amount of phase selectivity (F1/F0 $>$ 0.5) at high contrasts. Furthermore, they reported that, on average, the simple cell population did not change; however, individually some of their simple cells did show increases or decreases in F1/F0 that appear qualitatively similar to our results: 6/16 of their simple cells had F1/F0 ratios $<$1 at low contrast. In our study only a very small proportion of the neuronal population switched their cell type classification; the switch tended to be most frequent in the minority of cells that already contained a mixture of phase-selective and phase-invariant responses and only occurred at very low response rates. We interpret these findings to indicate that lowering of stimulus contrast is unlikely to substantially alter this property of cortical signaling.

We found that a large reduction in neuronal firing rates induced by presenting spatially extended stimuli had no effect on the F1/F0 ratio of neurons' responses in macaque V1, suggesting that the cellular classification established by local intracortical circuitry was not modified by strong activation of the eCRF. This is in marked contrast to the results of Bardy et al. (2006) in cat V1, which showed most complex cells (and some simple cells) increased their F1/F0 ratio with activation of eCRF suppression. The difference in results is unlikely to be due to sampling bias; most of our neurons were strongly suppressed by the stimuli of large size and spatial context, and the average amount and distribution of suppression across our population were similar to those of a large population of cells in another study (Cavanaugh et al. 2002a). Furthermore, we found no correlation between suppression strength and increase in F1/F0 ratio for complex cells. In the study of Bardy et al. (2006) the neurons showing strong increases had F1/F0 values in the range of 0.5–1.2 and thus contained a mixture of modulated and unmodulated responses. As we show in Fig. 3, this range is precisely where the dip occurred in our population distribution of F1/F0 values; thus, even if such cells showed a similar trend, it would be at most a minority of the V1 population. Additionally, many of the cells in the Bardy et al. study were suppressed such that they only fired a few spikes per second. As Crowder et al. (2007) showed and we confirmed, the F1/F0 statistic becomes biased at lowered firing rates. Bardy et al. (2006) did not take this bias into account, so there is the potential that some of their observed increase in F1/F0 was produced by lowered overall firing rates.

Implications for Visual Processing

The invariance of neuronal properties with contrast and context means that processing of images with different scene statistics can be processed in the same manner by the cortical population. It is of particular interest that simple cells, which comprise 50% of the population of 462 neurons we studied for contrast, were mostly stable in the F1/F0 ratio across a wide range of contrasts, suggesting that edge information conveyed by the simple cell population would be relatively constant independent of the local contrast of the edge. The implication for visual processing of an increased F1/F0 ratio for a small proportion of complex cells, about 13%, at near threshold contrast is difficult to predict. As pointed out earlier, neurons have different contrast thresholds, so although some of the 13% of complex cells that became more simple-like might potentially contribute to processing, they would have low spike rates, so their overall contribution to processing in the circuit might be relatively low. Consequently, in terms of visual processing, the ratio of simple-to-complex cell contribution in primates is relatively invariant with contrast and context.

GRANTS

This work was supported by National Eye Institute Grants EY017945, EY08300, and P31 EY-13079.

DISCLOSURES

The authors declare no competing financial interests.

AUTHOR CONTRIBUTIONS

C.A.H. and M.J.H. conception and design of research; C.A.H. and M.J.H. performed experiments; C.A.H. and M.J.H. analyzed data; C.A.H. and M.J.H. interpreted results of experiments; C.A.H. and M.J.H. prepared figures; C.A.H.

and M.J.H. drafted manuscript; C.A.H. and M.J.H. edited and revised manuscript; C.A.H. and M.J.H. approved final version of manuscript.

REFERENCES

Alonso JM, Martinez LM. Functional connectivity between simple cells and complex cells in cat striate cortex. *Nat Neurosci* 1: 395–403, 1998.

Bardy C, Huang JY, Wang C, FitzGibbon T, Dreher B. 'Simplification' of responses of complex cells in cat striate cortex: suppressive surrounds and 'feedback' inactivation. *J Physiol* 574: 731–750, 2006.

Bonds AB. Temporal dynamics of contrast gain in single cells of the cat striate cortex. *Vis Neurosci* 6: 239–255, 1991.

Cavanaugh JR, Bair W, Movshon JA. Nature and interaction of signals from the receptive field center and surround in macaque V1 neurons. *J Neurophysiol* 88: 2530–2546, 2002a.

Cavanaugh JR, Bair W, Movshon JA. Selectivity and spatial distribution of signals from the receptive field surround in macaque V1 neurons. *J Neurophysiol* 88: 2547–2556, 2002b.

Chance FS, Nelson SB, Abbott LF. Complex cells as cortically amplified simple cells. *Nat Neurosci* 2: 277–282, 1999.

Chen Y, Anand S, Martinez-Conde S, Macknik SL, Bereshpolova Y, Swadlow HA, Alonso JM. The linearity and selectivity of neuronal responses in awake visual cortex. *J Vis* 9: 12 11–17, 2009.

Crowder NA, van Kleef J, Dreher B, Ibbotson MR. Complex cells increase their phase sensitivity at low contrasts and following adaptation. *J Neurophysiol* 98: 1155–1166, 2007.

Dean AF, Tolhurst DJ. On the distinctness of simple and complex cells in the visual cortex of the cat. *J Physiol* 344: 305–325, 1983.

DeAngelis GC, Freeman RD, Ohzawa I. Length and width tuning of neurons in the cat's primary visual cortex. *J Neurophysiol* 71: 347–374, 1994.

Durand JB, Girard P, Barone P, Bullier J, Nowak LG. Effects of contrast and contrast adaptation on static receptive field features in macaque area V1. *J Neurophysiol* 108: 2033–2050, 2012.

Hawken MJ, Parker AJ, Lund JS. Laminar organization and contrast sensitivity of direction-selective cells in the striate cortex of the old world monkey. *J Neurosci* 8: 3541–3548, 1988.

Hawken MJ, Shapley RM, Grosof DH. Temporal-frequency selectivity in monkey visual cortex. *Vis Neurosci* 13: 477–492, 1996.

Hubel DH, Wiesel TN. Receptive fields and functional architecture of monkey striate cortex. *J Physiol* 195: 215–243, 1968.

Hubel DH, Wiesel TN. Receptive fields, binocular interaction and functional architecture in the cat's visual cortex. *J Physiol* 160: 106–154, 1962.

Levitt JB, Lund JS. Contrast dependence of contextual effects in primate visual cortex. *Nature* 387: 73–76 1997.

Mata ML, Ringach DL. Spatial overlap of ON and OFF subregions and its relation to response modulation ratio in macaque primary visual cortex. *J Neurophysiol* 93: 919–928, 2005.

Mechler F, Ringach DL. On the classification of simple and complex cells. *Vision Res* 42: 1017–1033, 2002.

Priebe NJ, Mechler F, Carandini M, Ferster D. The contribution of spike threshold to the dichotomy of cortical simple and complex cells. *Nat Neurosci* 7: 1113–1122, 2004.

Ringach DL, Shapley RM, Hawken MJ. Orientation selectivity in macaque V1: diversity and laminar dependence. *J Neurosci* 22: 5639–5651, 2002.

Sharpee TO, Victor JD. Contextual modulation of V1 receptive fields depends on their spatial symmetry. *J Comput Neurosci* 26: 203–218, 2009.

Skottun BC, De Valois RL, Grosof DH, Movshon JA, Albrecht DG, Bonds AB. Classifying simple and complex cells on the basis of response modulation. *Vision Res* 31: 1079–1086, 1991.

Tao L, Shelley M, McLaughlin D, Shapley R. An egalitarian network model for the emergence of simple and complex cells in visual cortex. *Proc Natl Acad Sci USA* 101: 366–371, 2004.

van Kleef JP, Cloherty SL, Ibbotson MR. Complex cell receptive fields: evidence for a hierarchical mechanism. *J Physiol* 588: 3457–3470, 2010.

Victor JD, Mechler F, Ohiorhenuan I, Schmid AM, Purpura KP. Laminar and orientation-dependent characteristics of spatial nonlinearities: implications for the computational architecture of visual cortex. *J Neurophysiol* 102: 3414–3432, 2009.

Webb BS, Dhruv NT, Solomon SG, Tailby C, Lennie P. Early and late mechanisms of surround suppression in striate cortex of macaque. *J Neurosci* 25: 11666–11675, 2005.

Wielaard DJ, Shelley M, McLaughlin D, Shapley R. How simple cells are made in a nonlinear network model of the visual cortex. *J Neurosci* 21: 5203–5211, 2001.

Williams PE, Shapley RM. A dynamic nonlinearity and spatial phase specificity in macaque V1 neurons. *J Neurosci* 27: 5706–5718, 2007.

Williams PE, Xing D, Yeh CI, Joshi S, Hawken MJ, Shapley RM. Laminar differences in complex cell dynamics in macaque V1. *Soc Neurosci Abstr* 279.6, 2007.

Xing D, Shapley RM, Hawken MJ, Ringach DL. Effect of stimulus size on the dynamics of orientation selectivity in Macaque V1. *J Neurophysiol* 94: 799–812, 2005.

Yeh CI, Xing D, Williams PE, Shapley RM. Stimulus ensemble and cortical layer determine V1 spatial receptive fields. *Proc Natl Acad Sci USA* 106: 14652–14657, 2009.

Zhu W, Shelley M, Shapley R. A neuronal network model of primary visual cortex explains spatial frequency selectivity. *J Comp Neurosci* 26: 271–287, 2009.